

Baseline aerial survey of fallow deer and forester kangaroo populations, Tasmania

Report to Tasmanian Department of Primary Industries, Parks, Water and Environment.

Mark Lethbridge, Michael Stead, Cameron Wells, Elen Shute
June 2020

This publication may be cited as:

Lethbridge, M.R., Stead, M.G., Wells C. and Shute, E.R. 2020. *Baseline aerial survey of fallow deer and forester kangaroo populations, Tasmania*. Report to Tasmanian Department of Primary Industries, Parks, Water and Environment.

EcoKnowledge

A trading name of Terrestrial Ecosystem Services Pty Ltd

ABN: 46 133 654 896

PO Box 632

Mylor 5153

Phone: 61-8-8388-5179

Fax: 61-8-8388-5794

www.ecoknowledge.com.au

Executive Summary

Background

Aerial survey data of fallow deer (*Dama dama*) and forester kangaroos (*Macropus giganteus tasmaniensis*) was collected in September and October 2019, using a helicopter seating up to three trained aerial observers per flight. We used two well-known aerial observation methods, namely Multiple Covariate Distance Sampling (MCDS) for forester kangaroos and Mark Recapture Distance Sampling (MRDS) for fallow deer. These were used to derive density and abundance estimates for these two species. For experimental purposes, we concurrently ran a FLIR™ T1K HD thermal camera to capture data on one side of the aircraft for comparison. MCDS was also applied to the thermal imagery detections.

Annual spotlight transect surveys have been the main method of monitoring deer populations in Tasmania to date. To determine how closely ground survey estimates matched aerial survey estimates of deer abundance and population density, we compared results from the aerial survey with spotlight data collected within two months of the aerial survey was used for comparison. A similar comparison for forester kangaroos was not possible due to very limited spotlight data for this species.

Results

The Mark-Recapture Distance Sampling (MRDS) of fallow deer in the aerial survey estimated an average population density over the study area of 2.696 deer per km² (CV 19%). Multiplied over the entire study area, this equates to an estimated population size of 53,660 deer in central and north-eastern Tasmania.

A different sampling method was used to estimate kangaroo population and density because a trainee observer, who flew 30% of the transects for training purposes, was restricted to counting deer only. For this reason, the Multiple Covariate Distance Sampling (MCDS) method was used to estimate forester kangaroo abundance and density, and found an average population density of 1.381 foresters per km² (CV 23%). Applied over the entire study area, this produced an estimated population size of 30,327 forester kangaroos in central and north-eastern Tasmania.

For comparison, an alternative statistic, the mark-recapture probability, was calculated for forester kangaroos for the 70% of flights where the trainee was replaced by a calibrated observer. If extrapolated over 100% of the study area, this would approximately double the estimated forester kangaroo population size, but this estimate is considered unreliable due to the extrapolation involved.

Spotlight trends

Population density estimates determined from spotlight data and aerial data were compared for fallow deer using a Kernel Density Estimator (KDE) mapping technique. There was a high degree of agreement between these density models, and therefore the aerial count from 2019 was used to retrospectively estimate population trends in fallow deer using

historical spotlight counts from 2016 to 2019. It is estimated that the deer population has increased by approximately 5.4% per year on average since 2016, even in the presence of removal effort (takes).

Simulations of spotlight data suggest that annual ground survey effort would need to be more than doubled in order to reduce variability in population density estimates to an acceptably low level (CV <25%).

Recommendations

- At least double current deer spotlighting effort to reduce CV
- Introduce distance sampling methods into spotlight surveys
- Trial the use of thermal binoculars in ground surveys
- Use occasional aerial surveys (4- to 5 year intervals) to calibrate ground survey data
- Trial the use of alternative aerial survey methods, including Unmanned Aerial Vehicles (UAVs) mounted with thermal cameras to determine effectiveness and cost-effectiveness.

Table of Contents

1.0	Introduction	6
2.0	Methods	6
2.1	Aerial survey area and transects.....	6
2.2	Aircraft operations.....	7
2.3	Mark-recapture Distance Sampling (MRDS) and Multiple Covariate Distance Sampling (MCDS).....	9
2.4	Thermal camera.....	11
2.5	Density distribution	11
2.6	Comparison with ground survey data	14
2.7	Modelling cost-effective future monitoring requirements	14
3.0	Results	17
3.1	Sightings of fallow deer and forester kangaroos	17
3.2	MRDS results – fallow deer.....	18
3.3	MCDS results – forester kangaroos.....	21
3.4	Density distribution of fallow deer	23
3.5	Density distribution of forester kangaroos	24
3.6	Comparison of fallow deer results with ground survey methods	24
3.7	Modelling future monitoring requirements – fallow deer	30
4.0	Discussion.....	31
5.0	Recommendations and future work	35
6.0	References	38

Appendix 1: Contours of aerial deer/km² anisotropic KDE

Appendix 2: Contours of spotlighting deer/km anisotropic KDE

Appendix 3: Contours of aerial deer/km² isotropic KDE

Appendix 4: Contours of spotlighting deer/km isotropic KDE

Appendix 5: Thermal survey trial

Appendix 6: Contours of aerial forester/km² anisotropic KDE

Appendix 7: Fallow deer - detailed outputs from Program Distance of MRDS $g(x) \sim \text{trainee} + \text{cluster size}$ $mr() \sim \text{trainee} + \text{cluster size} + \text{distance}$

Appendix 8: Forester kangaroos - detailed outputs from Program Distance of MCDS $g(x) \sim \text{cluster size}$

1.0 Introduction

Aerial surveys are a valuable method of estimating the distribution, density and abundance of medium to large mammals over wide geographical areas. In the context of game management, they can be designed to evaluate program performance, identify areas that trigger management actions, and provide a planning framework to optimise on-ground control.

The aim of the 2019 aerial survey was to determine the distribution, density and abundance of fallow deer (*Dama dama*) and forester kangaroos (*Macropus giganteus tasmaniensis*) in central and north-eastern Tasmania. The purpose of this information is to better inform future monitoring and management decisions for these species in Tasmania.

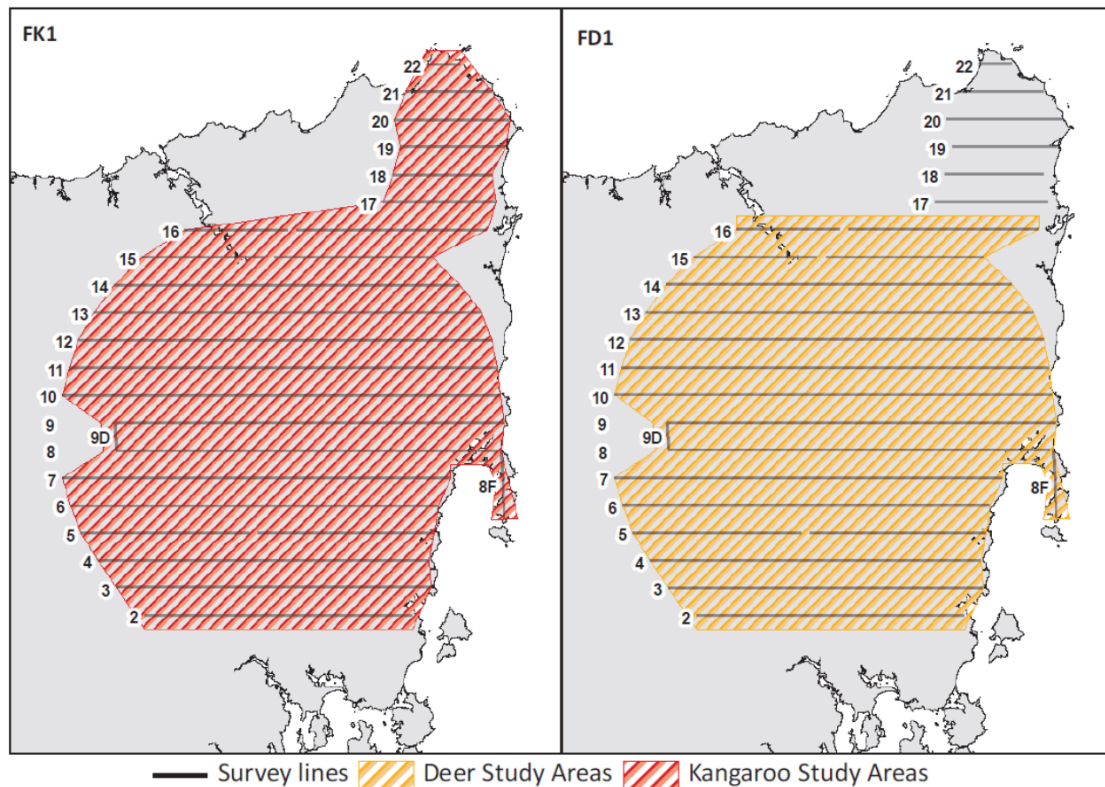
2.0 Methods

2.1 Aerial survey area and transects

An aerial survey was conducted over the central and north-eastern region of Tasmania from September 23rd – October 4th, 2019. Twenty east-west orientated transects and two small north-south transects were flown (Figure 1). The location and arrangement of the transects was negotiated with DPIWWE and based on current knowledge of the distribution of these species. The transects were spaced ~10 km apart north-south. The combined length of these transects was 2,170 km, over a total area of 21,958 km².

During the survey, minor deviations from transect were necessary to avoid conflicts with infrastructure (e.g. powerline and communications towers) and known nesting locations of the endangered Tasmanian wedge-tailed eagle (*Aquila audax fleayi*).

For the purpose of the analysis, the broader survey area was divided into two overlapping areas because the geographical ranges of fallow deer and forester kangaroos only partially overlap. The more extensive area (called FK1) occupies an area of 21,958 km² and was used to estimate the abundance of forester kangaroos. This meant transects 17–22 (the northernmost transects) were flown for the primary purpose of surveying forester kangaroos (Figure 1), and the northernmost region of the survey area was excluded from the deer analyses. The remaining area of 19,905 km² (called FD1), corresponding to transects 2–16, was used for the fallow deer analyses.



GDA 1994 MGA Zone 55

Figure 1 Transects flown during 2019 aerial survey and two areas used to calculate abundances (i.e. FK1 – forester kangaroos and FD1 – fallow deer).

2.2 Aircraft operations

All survey flights were conducted within three hours following first light and three hours preceding last light. This is the optimal time to conduct aerial surveys for crepuscular and/or nocturnal species such as deer and kangaroos, and is the common approach used for these species elsewhere in Australia for fixed-wing and helicopter manned operations. This is the time when these species are generally most active, at least during daylight hours when it is safe to fly. All transects (excepting 8F and 9D) were flown in an east-west direction to avoid observers looking into the sun. Un-forecast fog prevented transects 8 and 9 from being flown as far west as intended, when we had already committed to these two transect lines.

A Bell JetRanger (206) helicopter was provided by RotorLift. The helicopter flew at an average altitude of 200 feet (61 m) Above Ground Level (AGL) and held this height using a RADAR altimeter. The average survey speed was 50 knots (93 km h^{-1}).

Distance sampling (DS) involves mathematically modelling the decay in observer bias with the increasing perpendicular distance out from the aircraft (Buckland *et al.* 1993). Because the distance to each animal or group of animals cannot be directly measured in the air, the distance sampling methodology (and variants of DS – see later) accommodates the division

of each observer's view area into zones. These zones are delineated with graduated sighting poles mounted on the aircraft (Figure 2).

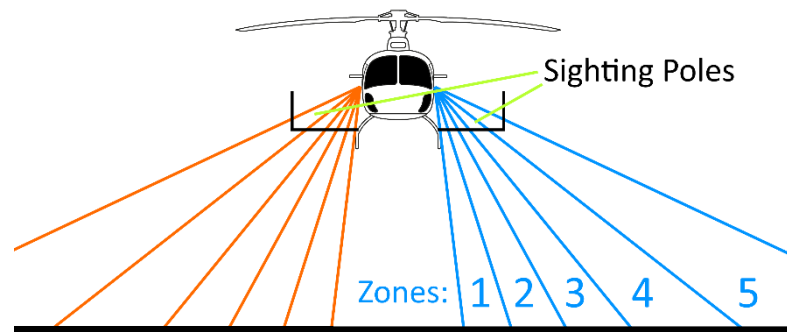


Figure 2 Delineation of sighting zones

A five-zone distance sampling approach was employed (0–20m, 20–40m, 40–70m, 70–100m, 100–150m) out of either side of the aircraft, based on the methods of Lethbridge *et al.* (2019) and using survey poles approved by a Civil Aviation Safety Authority (CASA) Engineering Order. The marked zones were calibrated against ground markers prior to commencement of the survey. All data were collected using eight-button electronic keypads attached to a Global Navigation Satellite System (GNSS). Buttons 1–5 were used to enter the number of individual animals counted in each of the five sampling zones. Buttons 6 and 7 were used to assign species (deer or kangaroo). The number of times buttons 6 and 7 were hit also recorded habitat structure (open, or medium to dense). Button 8 was used to remove erroneous entries. Importantly, after sufficient training, the keypad method means that observers do not need to look away from the viewing area to enter the data, and therefore improves count accuracy.

In summary, the following information was recorded on these keypads:

1. number of animals (grouped) and categorised into two species ('deer' or 'forester')
2. the zone (1, 2, 3, 4, 5) in which they were observed, and
3. habitat structure (open, medium to dense).

All keypad entries were stored in a single file for each survey flight. This file logged data from each keypad separately, with each data-point labelled with GNSS coordinates and time. When sighted, both species were recorded by observers in the zone they were first observed. From the air, observers differentiated forester kangaroos *Macropus giganteus* from other similar macropod species (e.g. Bennett's wallaby *Macropus rufogriseus*) by their size, shape, gait and responsive behaviour.

Two habitat types were defined and recorded: open habitats (with little to no canopy, including wetlands and paddocks); and medium to dense habitats, having either a closed canopy or an open canopy with a closed understorey (e.g. temperate rainforests).

The doors were removed from the aircraft to provide clear visibility of the ground to each observer. Sunglasses or tinted helmet visors were not used as these are known to reduce

visibility, particularly in wooded areas. For most of the flights, three calibrated surveyors were used at any one time, two positioned in the rear of the aircraft and one in the front-left seat. The calibrated observers were rotated through different seat positions between flights. Each calibrated observer had between 40 and 1200 hours of survey experience, with some having more than above 200 hours experience. All calibrated observers have previously been tested against a more experienced observer. For approximately 30% of the time, a trainee observer from DPIPWE participated in the flights. The trainee was always seated behind an experienced front-left observer for comparison. The trainee's counts were dealt with separately in a way so as not to downwardly bias the final results (see later).

Program *Export* (Lethbridge 2019) was used to export and combine the raw data from each observer, and for each flight. Distribution maps for fallow deer and forester kangaroos were created from the observation data.

2.3 Mark-recapture Distance Sampling (MRDS) and Multiple Covariate Distance Sampling (MCDS)

MCDS and MRDS use a detection function $g(x)$, which is the probability of detecting an object at distance x , the perpendicular distance out from the aircraft. It is assumed that $0.0 \leq g(x) \leq 1.0$. The equivalent probability density function fitted through a frequency histogram of observer observations is denoted $f(x)$.

The final density equation for one side of a transect line is given by Equation 1.

$$\hat{D} = \frac{n}{Lw\hat{P}} \quad \text{Equation 1}$$

Here \hat{D} is the density being estimated, n is the observed counts, L is the length of the sample area, w is the total width of the sample area, and \hat{P} is the overall probability that a randomly located object in the sample area is in fact detected (Buckland et al. 1993). This only accounts for perception bias. The product of \hat{P} and w is also known as the Effective Strip Width (ESW). ESW is the area under $g(x)$ curve outward from $x = 0$. This statistically derived metric is the effective perpendicular distance that observers see out from the aircraft. It is the distance at which the same fraction of animals is missed inside the ESW as observed beyond.

Detectability (or sightability) can also be affected by covariates like group size, observer position in the aircraft, sun direction and habitat (e.g. wooded versus open areas) as well as the perpendicular distance that animals are observed away from the aircraft. While generally minor, these effects may lead to a bias in the estimates of density and abundance (Laake et al. 2008; Pollock & Kendall 1987; Seber 1992). These variables were tested and assessed individually.

Akaike's Information Criterion (Akaike 1974) was used to rank all the models within a model set from 'best' to 'worst' relative to each other. The lowest AIC score indicates the best fitting model for the fewest parameters (known as model parsimony).

The coefficient of variation (CV), another indicator of a good model fit, was also calculated. The lower the CV value, the smaller the residuals relative to the predicted value. The CV is the ratio of the standard deviation to the mean. It provides a statistical measure of the dispersion (i.e. variability) around the mean and is commonly expressed as a percentage. Unlike MCDS, MRDS manages the issue that observers still do not see all animals, even if all animals close to the aircraft are sighted (described as $g(0) < 1$ - the fitting function or $p(0) < 1.0$). In other words there is not certainty that an observer sees an animal close to the aircraft (Pollock & Kendall 1987; Samuel et al 1987). The Mark Recapture (MR) component of MRDS involves modelling the difference between two observer counts on one side of the aircraft. Even if both observers are experienced, the front observer will at times, still see some animals not seen by the rear and vice versa. From these statistics an overall correction factor can then be calculated. This approach corrects the bias resulting from animals being missed that should theoretically have been visible – called perception bias. It does not correct for animals that are totally concealed and not visible to either observer – called availability bias (Marsh & Sinclair 1989).

MRDS combines MR with $g(x)$, the sightability decay function with distance >0 (Borchers *et al.* 2006). However, if the conditional probabilities between observers (i.e. the probability of Observer 1 sightings, given the probability of Observer 2 sightings, $p_{1|2}(x)$ and vice versa, $p_{2|1}(x)$) depart from the individual probability functions $p_1(x)$ and rear $p_2(x)$, there is reason to believe there is common dependency, i.e. both are changing with increasing distance out from the aircraft. Laake and Borchers (2004) firmly suggest in this case using a point independence modelling approach, rather than a full independence modelling approach because a full independence approach would otherwise be biased. Here the MR sub-model should have distance as a covariate, and by default the $g(x)$ sub-model in MRDS will also depend on distance. Both the MR sub-model and $g(x)$ can be separately modelled against other potential covariates influencing heterogeneity in the data.

MRDS was used to estimate density and abundance of fallow deer. It was not used to estimate density and abundance of forester kangaroos because the trainee observer in the left-rear position did not count kangaroos.

Grouping front and rear counts for MRDS

A simple 200-m tolerance was used to group front and rear observer counts. This considers the time delays between each observer entering the data, given the speed of the aircraft. If greater than 200 m, it was assumed any counts were not seen by both observers at the same time.

'Apparent' animal movement (often due to aircraft roll) can result in the front observer seeing a group of individuals in one viewing zone and the rear observer seeing the same group in an adjacent zone. We therefore applied the commonly-used practice of taking the first observer's distance as the distance of the object from the aircraft (Burt *et al.* 2014).

Analysis

Analyses were carried out using Program *Distance 7.2 Release 1* (Thomas et al 2010). This software identifies each group as a separate object, with the objects first modelled with distance x , in this case categorised into five viewing zones perpendicular to the aircraft track. For MRDS and MCDS, both the half-normal and hazard-rate functions were first tested without covariates. Then covariates were added in a stepwise approach. These included *group_size* (or cluster size), *habitat*, *trainee* and *sun_direction*. As the aircraft flew east-west transects early morning and later afternoon, the *sun_direction* covariate was divided into two categories: *sun_forward* and *sun-behind*. The covariate *trainee* was assigned a 1 if the trainee in the rear-left seat was present and 0 if this seat was occupied by a trained observer. For MRDS, the covariates were first tested for their contribution in the distance sampling component $g(x)$ of this method. The same covariates were then tested in the mark-recapture components.

2.4 Thermal camera

Use of thermal imaging for animal surveys such as this is largely untested, with few studies demonstrating unequivocal success. Because its use in this survey was experimental only, the thermal camera **Methods** and **Results** have been provided separately in Appendix 5. Animal counts generated using the thermal camera data are for research purposes only, and should not be relied upon, nor be cited in the scientific literature at this stage.

2.5 Density distribution

Since we had point location data for all sightings of fallow deer and forester kangaroos, we were able to use a commonly accepted approach to estimate density distribution of these species. This is effectively a 3D surface depicting how the density of these species change geographically. These density surfaces are generated using a Kernel Density Estimator (KDE - Silverman 1986), a popular method of estimating density for a range of applications in biology, geography, the environment, and the health sciences. It is best applied to describe the changing density of point locations of many animals across the landscape, not the historic locations of a single animal. KDE can readily be applied to sample data, in this case animal numbers sampled along a transect.

The Kernel Density Estimator takes many forms depending upon how its weight function is derived. These functions statistically derive the optimal density surface and strike a compromise between revealing both local and global trends in the data. The general form of the Kernel density equation is:

$$\hat{f}(X_j) = \frac{1}{nh^2} \sum_{i=1}^n k \left[\frac{x_i - X_j}{h} \right] \quad \text{Equation 4}$$

Here, x_i represents a vector. In this case the vector consists of an (X, Y) or $(East, North)$ ordinate pair for point i . Conversely, the vector X_j represents the coordinates of the centre of the j^{th} grid cell. In this grid cell we are estimating the local density of points in and around the cell, $\hat{f}(X_j)$. The value n is the total number of points in the study area and h represents a smoothing parameter (see below). Because X_i and x_i are vectors, $x_i - X_j$ represents the distance between the centre of our target cell (the j^{th} cell) and the i^{th} point.

$k \left[\frac{x_i - X_j}{h} \right]$ is a weight function that defines how the points around a location in the density surface (i.e. a grid cell at X_j) are weighted, which determines their relative contribution to the density estimate at grid cell X_j .

There are several different weight functions that have been employed in the literature, depending upon the application. In urban studies, the popular weight function is the Quartic Kernel or the Epanechnikov Kernel. This is used because it better deals with the (often) discontinuous nature of the urban landscape. In natural environments, a more appropriate weight function is the Gaussian (or Normal) weight function.

KDE Bandwidth

A KDE bandwidth determines the degree of smoothing applied to the surface that depicts the density distribution of animal sightings. The larger the bandwidth the smoother the surface. To calculate the bandwidth an object statistical approach must be taken. KDE has a statistical bandwidth h . This is effectively derived from the dispersion measured in the animal point locations. The most rigorous method is called the Least Squares Cross Validation method (LSCV – Silverman, 1986). The ‘Ad hoc’ estimate (Equations 4 and 5) is also a well-accepted approach and is a much easier and more intuitive way to calculate the bandwidth.

$$\text{Gaussian KDE 'Ad hoc' bandwidth} \quad h_{optimal} = \sigma_{xy} n^{-1/6} \quad \text{Equation 6}$$

Here σ_{xy} is the pooled standard deviation in the GPS coordinates of each animal and n is the total number of points.

The KDE is isotropic when it uses the pooled standard deviation. However, if the variance in the X and Y directions differ substantially, it may be better to smooth the density surface differently in these or other non-cardinal directions. For example, if the data were more dispersed in the Y direction, a smoother surface would be required. The anisotropic version of the KDE (employing the ‘Ad hoc’ method) alters the smoothing in each direction according

to the standard deviations (σ_x and σ_y) in the x and y directions respectively (i.e. the Easterly and Northerly directions).

Unfortunately when data is collected along transect lines, the 'Ad hoc' and LSCV bandwidth optimisation methods fail because the GPS points of deer and kangaroos data are artificially spread out in a north-south direction because the transects are spread out at 10-km intervals. This means, $h_{y,optimal}$ (north-south direction) is usually more inflated $h_{y,optimal}$ (east-west direction), thus artificially creating anisotropy.

2.6 Comparison with ground survey data

This survey is the first broad-scale baseline estimation of fallow deer and forester kangaroo distribution, density and abundance in Tasmania. As future monitoring needs to be cost-effective and inform management, it is necessary to compare aerial survey data with existing and cheaper forms of monitoring, to ascertain what combination of methods is appropriate to monitor populations in coming years.

Initially it was intended that the aerial survey data would be compared with ground survey data for both deer and kangaroos. Walking transect survey data for forester kangaroos was provided by Game Services Tasmania, but as this only covered a small area of the aerial survey it was decided not to attempt to compare this data with the aerial survey data. The aerial versus ground survey data comparison therefore focuses on the much more extensive deer spotlight data.

Driving spotlight transect data of deer was well distributed over the survey area. This dataset extended back to 1975 and was provided by Game Services Tasmania. The dataset consists of 90 transects in the FD1 aerial survey area, each approximately 10 km long. As the 2019 data was collected within two months of the aerial survey, estimates of deer per kilometre length from these transects were compared with the aerial survey densities from the same area.

While it is tempting to derive a scale factor between the average number of deer per kilometre from the spotlight transects and deer per km² from the aerial survey, since the aerial survey was not flown prior to 2019, there is no way to determine if the two methods have reliably agreed at varying deer densities within the same geographical location over time. This would first need to be proven before a reliable link between the methods could be ascertained. As an alternative, we tested the relationship between varying deer densities over geographical space in 2019 using two KDE surfaces, one derived from the spotlight transect and the other from the aerial survey data.

2.7 Modelling cost-effective future monitoring requirements

As previously mentioned we were unable to directly compare forester kangaroo data with the aerial survey data. Instead we focused on the deer spotlighting data and later draw inferences about possible future monitoring scenarios of forester kangaroos based on the fallow deer survey data. For deer we confined our temporal analysis to the period 2006–2019, as this was thought to be most relevant in considering future monitoring and management.

When monitoring native and introduced species, it is important that land managers set appropriate tolerances on the precision they are prepared to accept in their data. In kangaroo management in Australia, most jurisdictions set a coefficient of variation (CV) of

25%. This is the precision (an error tolerance) in abundance estimates, which needs to be considered when setting removal targets. These are only estimates of the random errors (or variations) presented in the data, in the absence of knowing the true population. They do not capture any undetected systematic biases.

As a general rule, for the same sampling effort, as the population increases, the statistical power will also increase. This often means the magnitude of the CV will reduce. This is providing there is no increase in clumping in the data (e.g. when the animals form larger herds/mobs), which may increase the CV.

Package *DSsim* (Marshall 2020) offers an approach to test surveys designs against a desired precision (i.e. the Coefficient of Variation - CV). While *DSsim* provides the most comprehensive analysis compared with other packages (for example, the ability to use past survey results, import transect data and simulate hotspots), it requires the *Distance* software to generate models as binary objects in advance. It does not facilitate for MRDS sampling.

Therefore, in this study we used a package called *Aerial and ground survey CV simulator* (Lethbridge 2015). As inputs, this requires a KDE surface of known density hotspots, the average and Standard Deviation (SD) of group sizes, a maximum group size, the effective strip width and an estimation of detectability, together with its variance. The software pseudo-randomly locates groups of animals of varying group sizes, according the average group size and SD, and according to the KDE density surface. This is repeated in each simulation sequence.

The Graphical User Interface (GUI) of *Aerial and ground survey CV simulator* is shown in Plate 1. A CV is calculated for each simulation using an ESW (and SD) and, where appropriate a MR probability and SD. These data are usually obtained from past surveys in the same or similar landscapes. An average CV is then calculated over many simulations. This application has been tested against a large number of survey estimates of CV by the authors and has remained within 3% of CV estimates, providing group sizes and their associated variances have been similar.

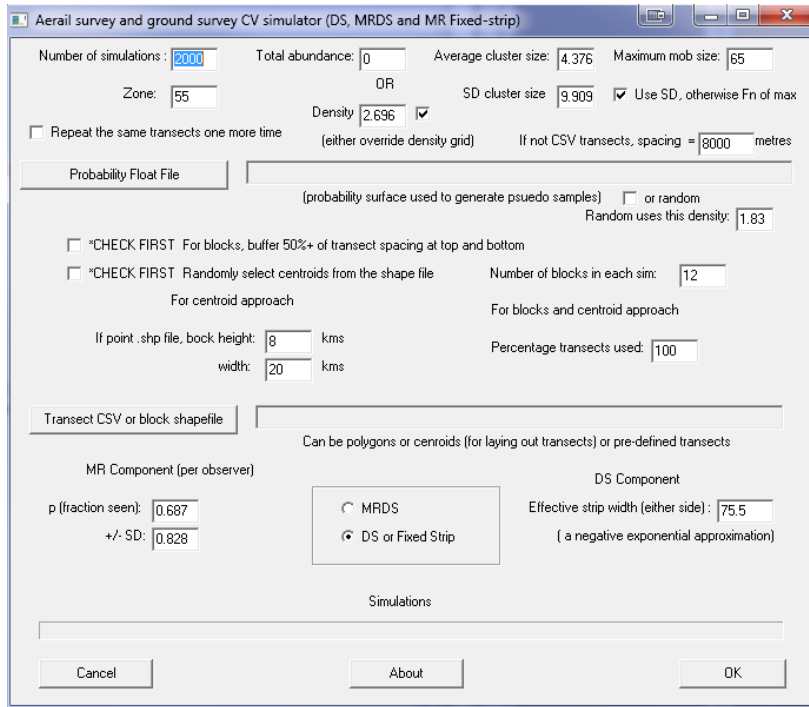


Plate 1 Graphical user interface of *Aerial and ground survey CV simulator* (Lethbridge 2015).

3.0 Results

3.1 Sightings of fallow deer and forester kangaroos

The aerial survey sightings of fallow deer (Figure 3) appear to extend from Launceston southward along the South Esk River corridor and through the Midlands to south of Ross. Populations extend up onto the Central Plateau and downs towards Bothwell and Hamilton. No deer were sighted in the northwest region.

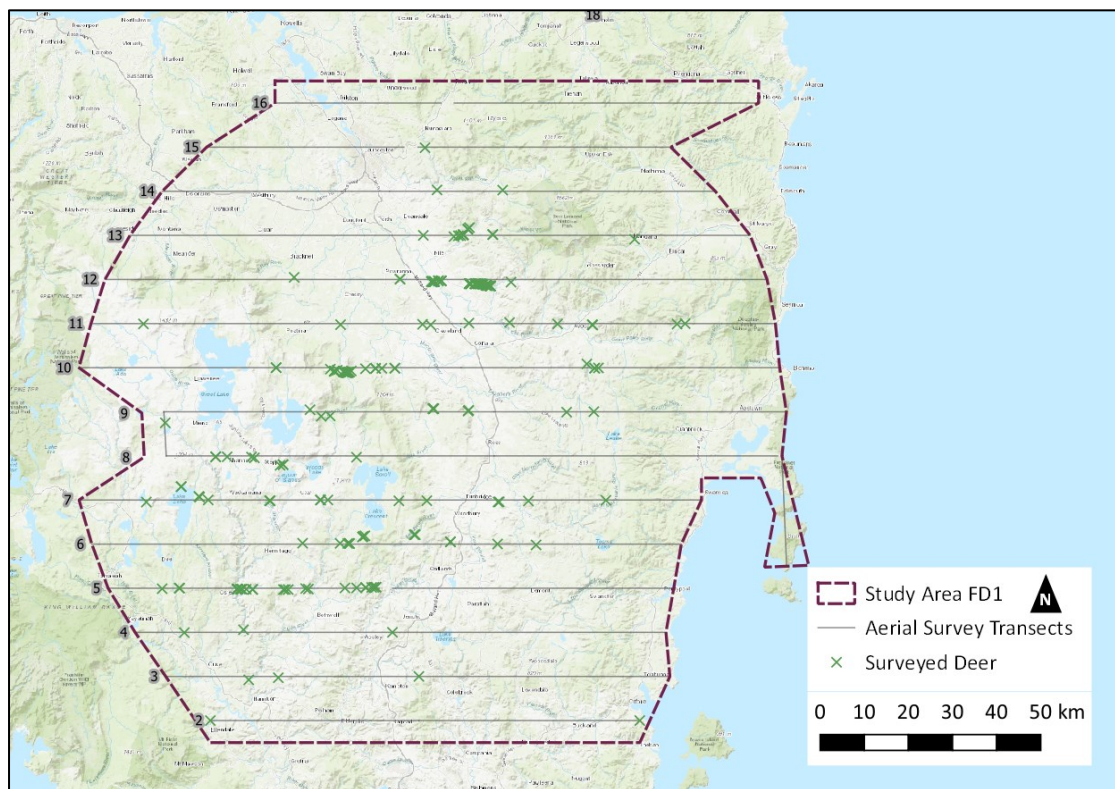


Figure 3 Fallow deer sightings based on observer counts (green crosses)

Forester kangaroos (Figure 4) were more broadly distributed across the survey area in lower numbers, including the upper Northwest. This species was largely absent from the Central Plateau.

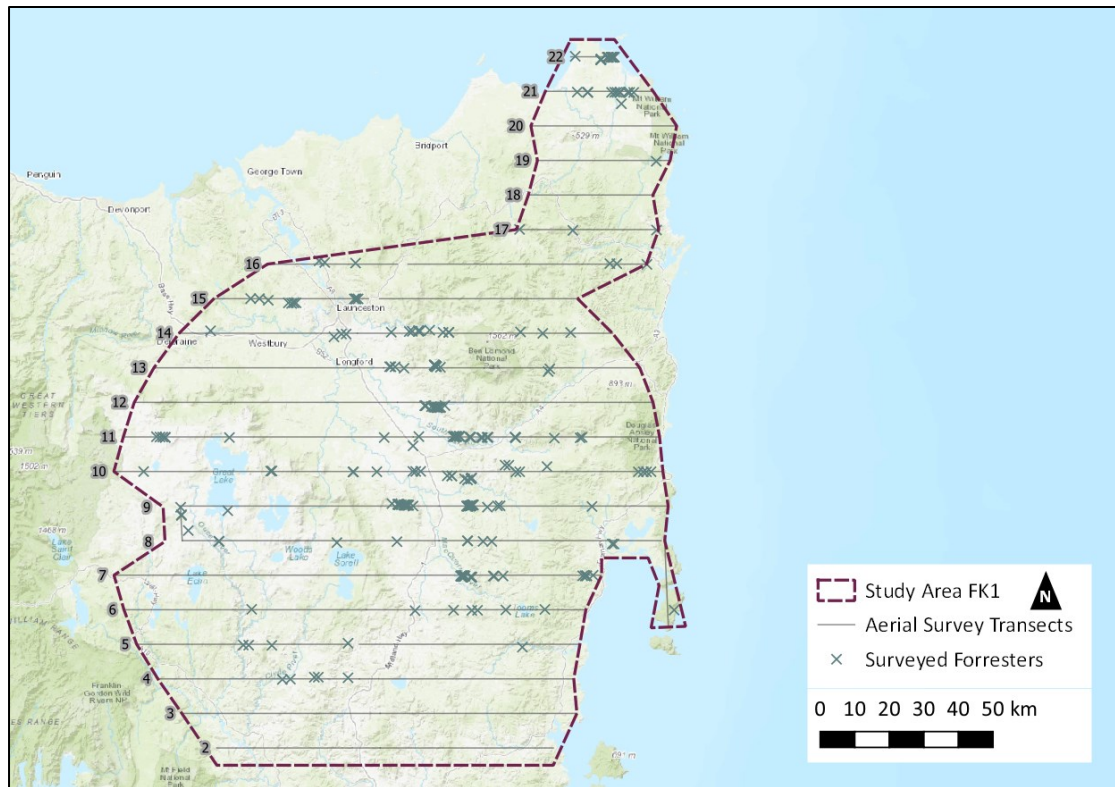


Figure 4 Forester kangaroo sightings based on observer counts (dark green crosses).

3.2 MRDS results – fallow deer

As we had a trainee seated behind the front-left observer for ~30% of the survey, the best way to manage any biases associated with the trainee’s counts was to test ‘trainee’ as a covariate in the model, in an attempt to explicitly model any biases from this person out of the results. As before, the ‘trainee’ covariate variable is given a ‘1’ when the trainee is present in the rear-left seat and a ‘0’ when a calibrated observer was present in the rear-left seat.

Figures 5 and 6 show the probabilities and conditional probabilities best summarise a comparison of the front and rear observers. The conditional probabilities between observers $p_{1|2}(x)$ and $p_{2|1}(x)$ in Figure 6 are relatively flat lines and depart from the individual probably functions $p_1(x)$ and rear $p_2(x)$ in Figure 5. They are however, very close in magnitude at $p(0)$. This shows some dependency between front and rear positions with distance out from the aircraft because they do not follow the same shapes as Figure 5. This suggests using a Point Independence (PI) modelling approach, rather than a full independence modelling approach because while there appears to be independence at $x = 0$ (i.e. the same probabilities are apparent between Figures 4 and 5 at $x = 0$), the flatter lines in Figure 6 show a positive correlation between observers, thus a full independence approach would be biased at larger distances (Laake and Borchers 2004).

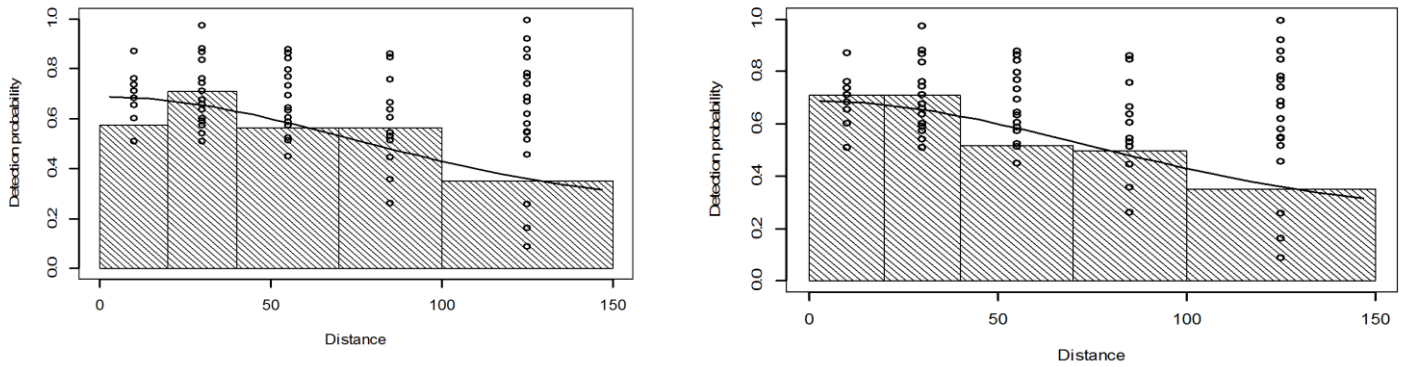


Figure 5 Front $p_1(x)$ and rear $p_2(x)$ detection probabilities respectively

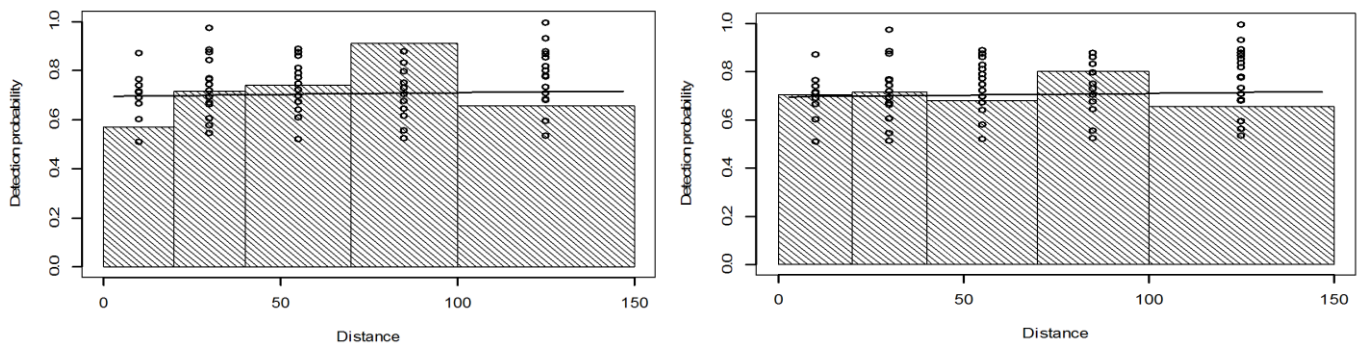


Figure 6 Front detection probabilities given the rear $p_{1|2}(x)$ (left), and rear detection probabilities $p_{2|1}(x)$ given the front (right).

Table 1 shows the relative performance of models with each combination of covariates using the MRDS approach. We followed the approach taken by Borchers et al. (1998), where the DS and mark-recapture components of MRDS both depended. Table 1 also shows other covariates we tested, which may explain data heterogeneity. For the mark-recapture component, distance is only treated as a linear covariate of sighting probability (Becker and Christ 2015). From Table 1, the best scoring MRDS model for the FD1 area with the lowest AIC score was $g(x) \sim \text{trainee} + \text{cluster size}$ and $mr() \sim \text{trainee} + \text{cluster size} + \text{distance}$. The **trainee** covariate is 1 when the trainee was present and 0 when they were not. This was found to be important in the model, suggesting the presence of the trainee could have biased the results if not considered. Group size (cluster size) also affected sightability. Here the density estimate was 2.696 deer per km² (CV 19%; LCL 1.839; UCL 3.952). Appendix 7 shows more detailed outputs of the best performing model from Program *Distance*.

Table 1 MRDS models tested for fallow deer in FD1 area

<i>Model</i>	<i>AIC</i>	<i>D</i>	<i>LCL</i>	<i>UCL</i>	<i>CV</i>
$g(x) \sim \text{trainee} + \text{cluster size}$ $mr() \sim \text{trainee} + \text{cluster size} + \text{distance}$	751.9	2.696	1.839	3.952	19%
$g(x) \sim \text{trainee} + \text{cluster size} + \text{habitat}$ $mr() \sim \text{trainee} + \text{cluster size} + \text{distance}$	754.4	3.129	0.005	NA	19%
$g(x) \sim \text{cluster size} + \text{trainee}$ $mr() \sim \text{distance}$	759.0	2.775	1.874	4.118	19%
$g(x) \sim \text{trainee}$ $mr() \sim \text{trainee} + \text{distance}$	761.9	3.203	2.087	4.916	21%
$g(x) \sim \text{cluster size} + \text{trainee} + \text{sun}$ $mr() \sim \text{distance}$	762.9	2.591	1.756	3.822	19%
$g(x) \sim \text{trainee}$ $mr() \sim \text{distance}$	763.9	3.182	2.066	4.896	21%
$g(x) \sim \text{trainee} + \text{sun}$ $mr() \sim \text{distance}$	764.1	3.247	2.066	5.102	22%
$g(x) \sim \text{sun}$ $mr() \sim \text{trainee} + \text{distance}$	764.2	3.177	2.054	4.914	22%
$g(x) \sim .$ $mr() \sim \text{distance}$	765.3	3.097	2.021	4.745	21%
$g(x) \sim \text{trainee} + \text{sun}$ $mr() \sim \text{position} + \text{distance}$	766.1	3.247	2.066	5.102	22%
$g(x) \sim \text{sun}$ $mr() \sim \text{distance}$	766.2	3.137	2.031	4.848	21%

Abbreviations: AIC (Akaike's Information Criterion); D (density km²), CV (coefficient of variation); LCL (lower confidence interval); UCL (upper confidence interval).

Table 2 Best scoring fallow deer models (FD1 area), together with density estimates (to 3 decimal points) and abundance estimates.

FD1 Area (km²)	Density	Abundance	CV
19,905	2.696	53,660	19%

Using the best scoring model with the lowest AIC score (bolded in Table 1), the estimated abundance of fallow deer in area FD1 is 53,660 (Table 2).

For this model, Figure 7 shows the pooled detection probability of both observers with distance. As expected, the line of best fit shows $g(x)$ decaying with distance out from the aircraft.

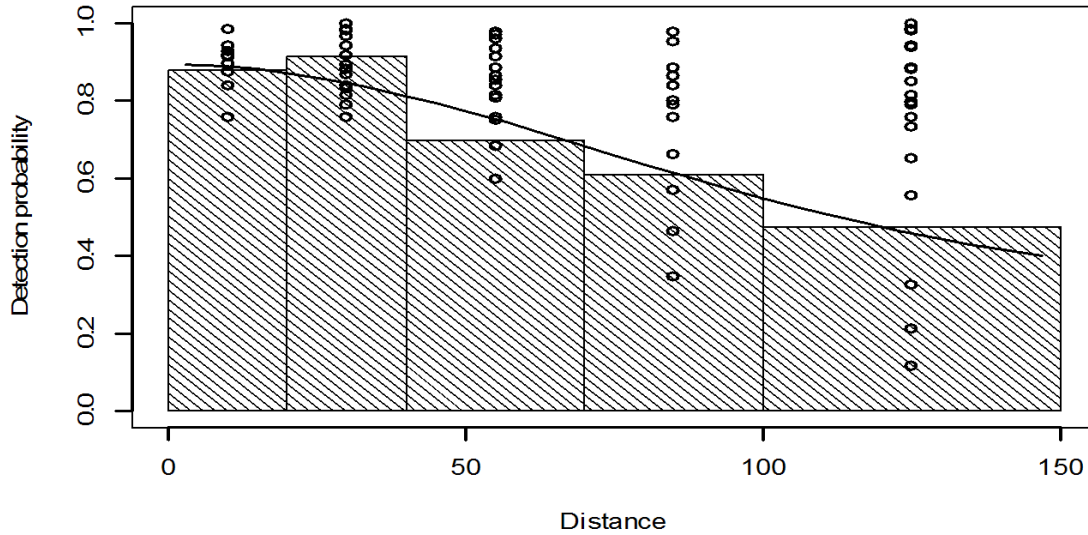


Figure 7 Pooled detection probabilities with distance (m).

3.3 MCDS results – forester kangaroos

MCDS was used to estimate density and abundance of forester kangaroos in the FK1 area, using animal counts by the front-left and rear-right observers. The MCDS models tested are shown in Table 3. We tested the effects of different combinations of cluster size, the direction of the sun, observer position in the aircraft, and habitat. We used a hazard rate model, which is more able to smooth out the effects of flushing that are more apparent with forester kangaroos. Figure 8 shows that sightability, or $g(x)$, decayed in zone 5, furthest out from the aircraft. Although there were fewer kangaroos seen in zone 1 (0–20 m), more were seen in zone 2 (20–40 m). In this case $g(x)$ smooths out the differences between the two.

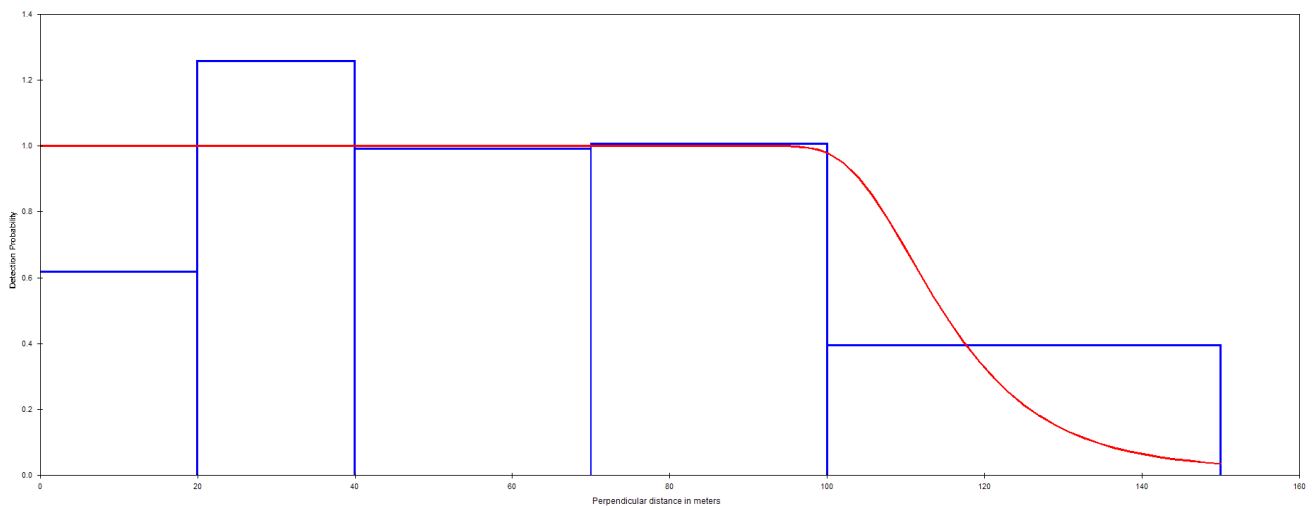


Figure 8 Combined front-right and rear-left detection probabilities with distance. Red line represents $g(x)$, or sightability decay with distance.

The best model in Table 3, having the lowest AIC score, was $g(x) \sim \text{cluster size}$. Thus cluster size (the group size of kangaroos) is the covariate that best explains the heterogeneity in the data. Appendix 8 shows more detailed outputs of the best performing model from Program *Distance*.

Table 3 MCDS models tested for forester kangaroos in the FK1 area

<i>Name</i>	<i>AIC</i>	<i>D</i>	<i>D LCL</i>	<i>D UCL</i>	<i>D CV</i>
$g(x) \sim \text{cluster size}$	789.9	1.381	0.872	2.186	23%
$g(x) \sim \text{cluster size} + \text{sun}$	791.9	1.381	0.872	2.186	23%
$g(x) \sim \text{cluster size} + \text{habitat}$	794.2	1.436	0.907	2.274	23%
$g(x) \sim \text{habitat}$	795.4	1.404	0.887	2.223	23%
$g(x) \sim \text{position}$	795.4	1.382	0.873	2.188	23%
$g(x) \sim \text{cluster size} + \text{habitat} + \text{sun}$	795.6	1.427	0.901	2.261	23%
$g(x) \sim \text{cluster size} + \text{sun} + \text{habitat} + \text{position}$	795.8	1.402	0.886	2.220	23%
$g(x) \sim \text{habitat} + \text{sun}$	797.1	1.400	0.884	2.217	23%
$g(x) \sim \cdot$	800.7	1.549	0.968	2.480	24%
$g(x) \sim \text{sun}$	802.5	1.550	0.978	2.458	23%

Abbreviations: AIC (Akaike's Information Criterion); ESW (effective strip width); D (density per km²); LCL (lower confidence interval); UCL (upper confidence interval); CV (coefficient of variation)

Using the best scoring model the abundance of forester kangaroos was calculated by multiplying the density of 1.381 (Table 4) by the total area of FK1. This gives an abundance of 30,327.

Table 4 Best scoring forester kangaroo models (FK1 area), together with density estimates (to 3 decimal points) and abundance estimates.

FK1 area (km²)	Density (animals per km²)	Abundance estimate	CV
21,958	1.381	30,327	23%

Mark-recapture alternative

For comparison, an alternative mark-recapture probability $p(0)$ was calculated from the two trained observers on the left-hand side of the aircraft, and its invert multiplied by the abundance estimate in Table 4. This statistic describes the front and rear observers' perception bias, but was calculated only for the 70% of the survey when the trainee was not present. Adopting $p(0)$ from the first 70% of the survey and applying it to the whole survey

is, in effect, an extrapolation and assumes that throughout the flight, the conditions affecting $p(0)$ are the same. This may compromise its validity and as such we believe it to be less reliable than desirable. Nevertheless, by way of comparison only, we show the effect of carrying out this adjustment.

After testing a number of covariates including habitat, sun direction, cluster size and distance, the best mark-recapture model was $mr() \sim \text{cluster size}$. In other words, the distance out from the aircraft did not affect the conditional probabilities between the front and rear observers. Here $p(0) = 0.493$. The invert of 0.493 (2.028) is the multiplication factor, assuming this was the same throughout the flight. If adopted, this would increase the estimate of forester kangaroo abundance from 30,327 to 61,516.

3.4 Density distribution of fallow deer

Two outliers were identified in the density data. These occurred when large group sizes of more than 50 individuals were sighted because the animals had at that moment of flight formed large groups. This has the potential of artificially inflating the density surface over the surrounding geographical area, thus they were removed.

After removal we then tested the difference between the variances in the East coordinates compared with the variance in North coordinates in the aerial survey points where deer were seen. These two variances were tested using an F-statistic. They were found to be significantly different ($\alpha=0.05$), thus anisotropy is apparent in the data (see Table 5). This requires the bandwidth in each cardinal direction to be calculated separately. These were $h_{x,optimal} = 10,266$ (the Easterly direction) and $h_{y,optimal} = 12,216$ metres (the Northerly direction) respectively.

Table 5 F statistic of variances in the East and North coordinates of aerial survey points

	<i>Easterly</i>	<i>Northerly</i>
Mean	518142	5356769
Variance	619411811.3	8.77E+08
Observations	203	203
df	202	202
F	0.706	
P(F<=f) one-tail	0.007	
F Critical one-tail	0.793	

Using Program *Kernel* (Lethbridge 2015), a KDE density surface was then created over the FD1 area to show the changing distribution of fallow deer. This is shown in Appendix 1. The average density of the density surface is 2.696 deer per km² (the MRDS estimate from Table 1).

The average number of deer per kilometre across all 88 transects was 0.629. Again two outliers were identified in the spotlighting data, where an unusually high number of deer were seen (7.4 per km at Lake Sorell 3 [LS3] and 12.4 per km at Waddamana 2 [WA2]; see Figure 9). These were removed from the data for the same reasons mentioned in 3.4, leaving an average of 0.417 deer per km (see later). The average density of deer over FD1 using the aerial survey MRDS method was 3.170 deer per km². As previously mentioned, while it is tempting to derive a scale factor between methods (in this case simply dividing the average deer per km from the 88 spotlight transects), since no aerial survey had been flown prior to 2019, there would be no way to determine if the two methods reliably agree over time. Instead, to investigate whether there is a reliable link between the two methods, we tested their relationship for varying deer densities over geographical space in 2019, acknowledging some deer movement may have occurred between the aerial survey and spotlight transects.

The deer per km estimates from spotlight transect were stored at the centroids (a single central coordinate) along each transect line. Using these points, we calculated a KDE surface, this time depicting a surface over the FD1 area of the number of deer sighted per km driven.

After outlier removal, the 'ad hoc' estimation of $h_{x,optimal}$ and $h_{y,optimal}$ were 19,261 and 23,938 metres respectively for the spotlighting data of deer. When we tested the difference between the variances in East coordinates compared with North coordinates using an F-statistic. They were found to be significantly different ($\alpha=0.05$), hence anisotropy was detected in the spotlight data (Table 6). Once again this requires the bandwidth in each cardinal direction to be calculated separately. The final anisotropic KDE surface for deer per km from spotlight transects is shown in Appendix 2.

Table 6 F Statistic of variances in the East and North coordinates of spotlight transect centres

	<i>Easterly</i>	<i>Northerly</i>
Mean	537803.7447	5367228.209
Variance	1643865246	2539197367
Observations	87	87
df	86	86
F	0.647395617	
P(F<=f) one-tail	0.022620291	
F Critical one-tail	0.699977513	

Comparing KDE surfaces

When comparing two or more KDE surfaces, for consistency the bandwidths of the two surfaces need to be the same. Otherwise the differences in the surfaces may be an artefact of differences in the bandwidths and not real changes in deer distribution (Ratcliff and McCullagh 2005; Fotheringham et al 2002). Anisotropy also confounds this. We therefore compared the surfaces using an average isotropic bandwidth for both surfaces.

Using the 'ad hoc' bandwidth calculations for both surfaces above, the average bandwidth ($h_{optimal}$) in the x and y direction of both datasets is 16,420 metres. We then applied this single bandwidth to create new isotropic KDE surfaces for aerial survey and spotlighting data (see Appendix 3 and 4).

The two density surfaces based on data from each method were directly compared at 1,000 random locations to see if there was a correlation between deer per km estimates from the ground with deer per km² estimates from the air. The correlation was found to be significant between these two surfaces, sampled at 1,000 random points ($F = 5291.4$, $p = 0.00$, $\alpha = 0.05$, $R^2 = 0.84$). The slope of the regression line is a scale factor relating the spotlight estimates the aerial survey. This was 0.151 +/- 0.002 Standard Error (SE), which is in the units of kilometres. Interestingly, this is an indirect way to estimate the average effective strip width of the spotlight transects (151 metres). Since vehicle spotlighting is conducted on both sides of the vehicle, and the figure of 151 metres refers to the total viewing area, half this width either side of the vehicle is ~76 metres.

Trends over time in spotlighting data

Assuming 151 metres has been consistent over time, we then multiplied this strip width by all deer per km calculations from the spotlighting time series from 2006 to 2019. We then multiplied these results by the total area of FD1 (19,905 km²) to estimate abundances over time (Figure 11).

Driessen et al. (1992) reported that dry conditions appeared to upwardly bias the number of deer seen because more animals are seen foraging more widely in open areas for feed. We also found this relationship (Figure 10). While a range of rainfall periods were assessed, the total rainfall which fell over the four months prior (including the month spotlighting was conducted) had the highest correlation (Figure 10). There was a negative correlation between this rainfall period and the number of deer seen. In other words, more deer are seen in dryer conditions. The slope of this line and F statistic were significant ($F = 10.29$, $p = 0.008$, $\alpha = 0.05$, $R^2 = 0.46$).

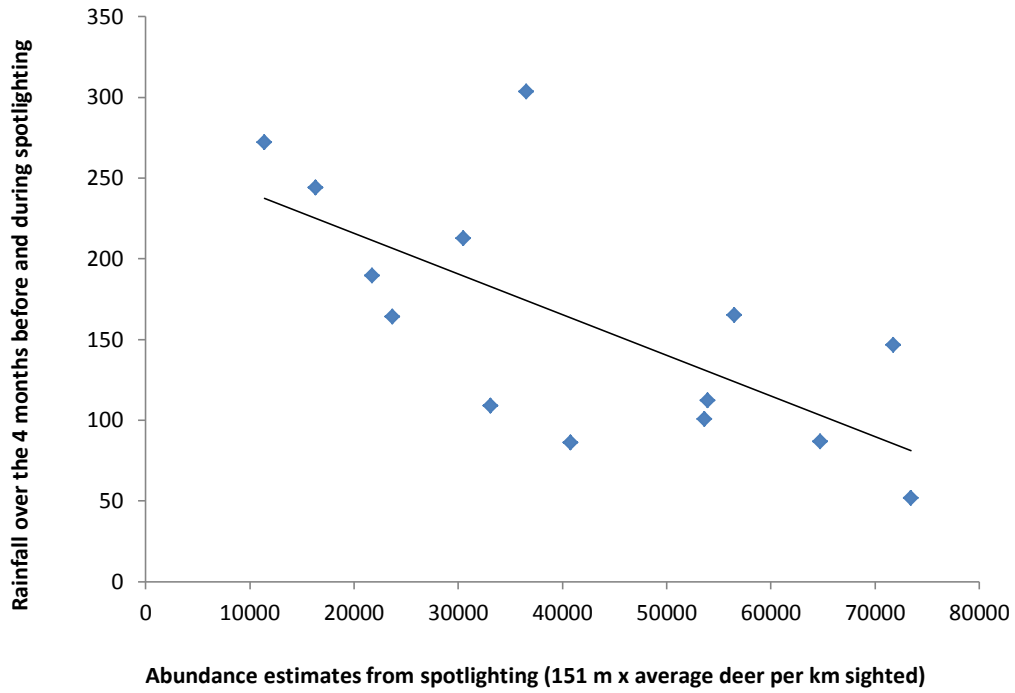


Figure 10 Spotlight transect abundance estimates versus the prior 4 months of rainfall

In Figure 11, deer abundance estimates from spotlighting using the 151-metre strip width have been corrected for these rainfall effects. Corrected estimates are shown as grey bars. As these are recorded in November each year, Figure 11 shows the annual reported take data provided by Game Services Tasmania from hunting and farm permits of the same year added to these bars (pink bars).

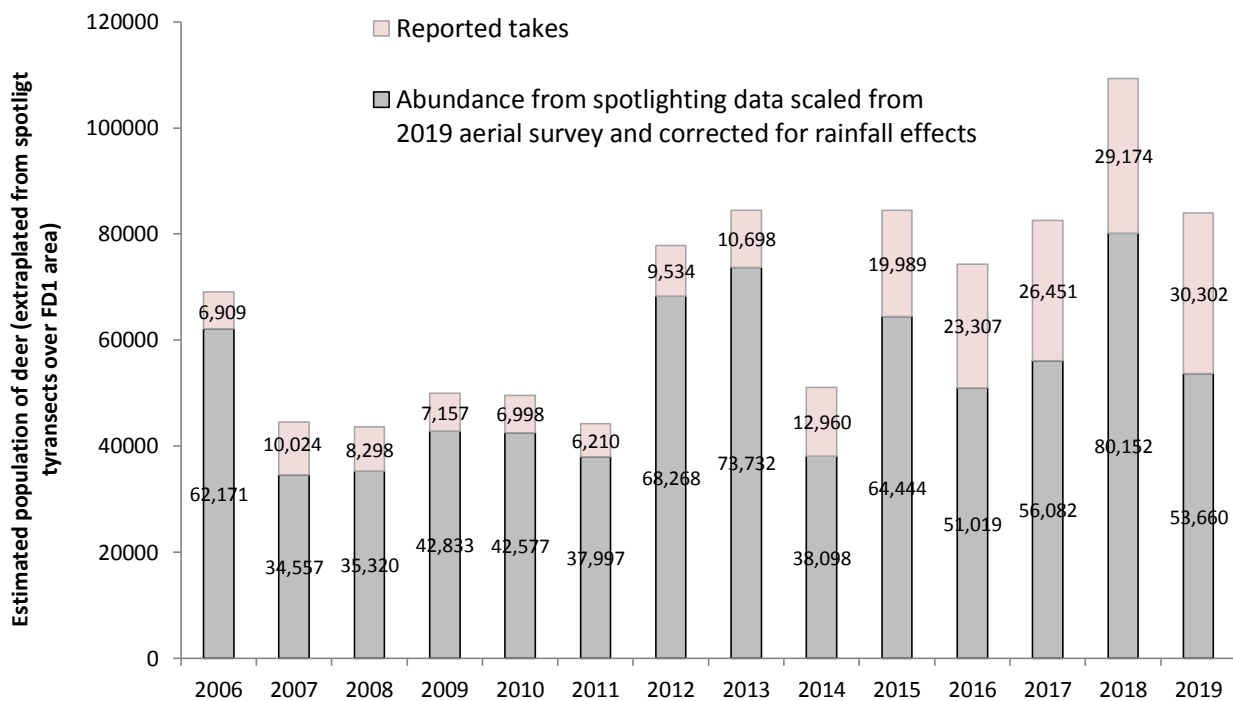


Figure 11 Spotlight transect abundance estimates in November each year, added to deer take (removal) data over that year.

A regression fit of the natural log of the addition of the spotlight estimates and the removals each year, gives a slope of 0.053 ($F = 12.84$, $p = 0.004$, $\alpha = 0.05$, $R^2 = 0.52$). The exponent of the slope of 0.053 is 1.054, which is a coarse measure of the rate of increase of the net population. The population increase figure of 1.054 is coarse because it is affected to some degree by temporal autocorrelation and is potentially affected by environmental stochasticity (McCullum 2000). Nevertheless, it suggests that the fallow deer population in north-eastern Tasmania has increased by approximately 5.4% per year on average between 2006 and 2019, even in the presence of removal effort (takes), although more recent takes from 2015 appear to be holding the population at a steadier state than prior to 2015.

However, 1.054 is not the natural population growth rate. Natural population growth is the growth rate in the absence of removals. This is difficult to estimate, but to gain some understanding of its magnitude, we added reported removals for each year to the spotlighting estimates, and then divided this sum by the abundance estimate from *spotlighting only* in the previous year. Each of these ratios represents what the change in abundance over a year would have been if there had been no removals.

We then calculated the natural logarithm of these ratios to derive ' r ', an estimate of the natural rate of increase (see McCullum 2000). Removals alter the demographic structure of most populations, often decreasing their breeding potential, so the average of these annual

estimates ($r = 0.240$) is likely to be a conservative estimate. The exponent of 0.240, that is, the rate of increase from 2006 to 2019, is 1.27. In other words, the natural population growth rate of fallow deer is likely to be more than 27% per annum, compared with the net population growth rate after removals, which is closer to 5% per annum.

Variance in the population growth rate results from the combination of demographic and environmental stochasticity, exacerbated by observation error. In the absence of detailed demographic data, long-term population trends can often provide some insights about these processes. For example, comparing abundance with population growth rate can help detect density-dependence (i.e. whether limited resources are reducing the population; Lande *et al.* 2003, 2009). However, there was no evidence of this in the spotlighting data. There was also no evidence of environmental autocorrelation in the data.

Using the **Lev (1962) numerical response equation**, we modelled the effect of rainfall on the rate of increase each year as estimated from spotlight data, using Bureau of Meteorology rainfall data collected at Ross. We tested a wide range of rainfall intervals for a range of temporal lags more than four months prior to each spotlight survey so as not to conflict with the four months of rainfall we already found negatively correlated with spotlight counts. **We found that the cumulative rainfall from January to July each year had the best relationship with r , the natural rate of increase estimate defined above. However, this was still weak with no statistical significance ($R^2 = 0.26$ – Figure 12).**

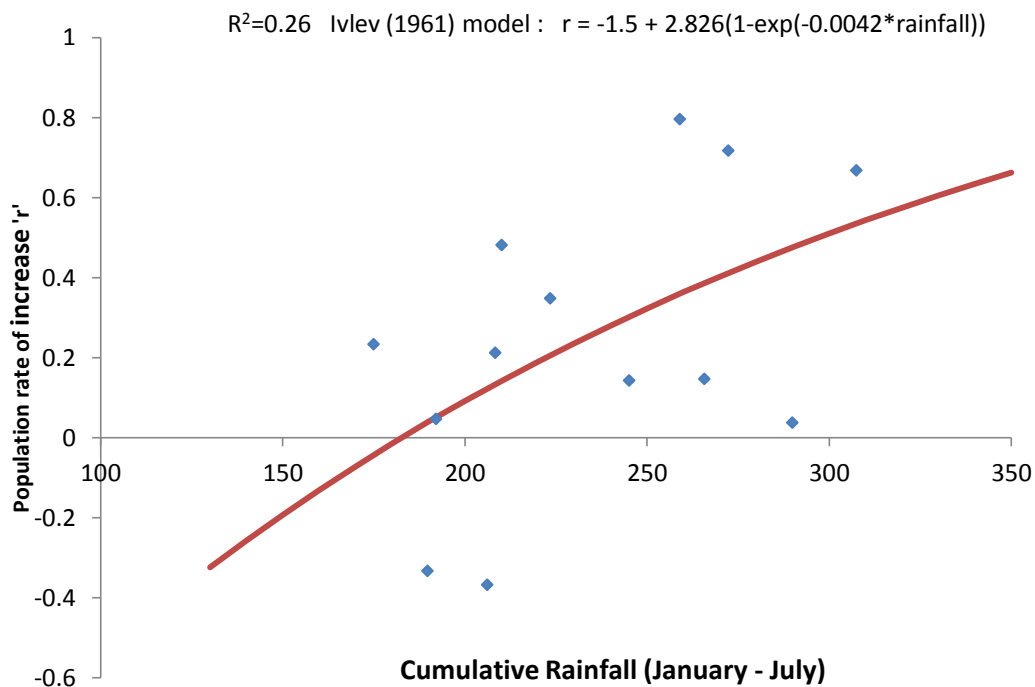


Figure 12 Weak relationship between the January to July cumulative rainfall each year and the annual rate of increase of deer.

3.7 Modelling future monitoring requirements – fallow deer

Both the observed population growth rate and the natural population growth rate of fallow deer appear to be increasing over time, with no evidence of density dependence and only a weak relationship between rainfall and fallow deer population growth.

This is important for assisting in the determination of how deer should be monitored into the future. In the absence of other supporting information, we assume that the current population estimate of 53,660 from the aerial survey is a reasonable minimum to determine future monitoring needs, providing that the size of groups of deer (the level of clumping) remains the same into the future. If the current 19% CV for this estimate is acceptable, this suggests that the current aerial survey effort as designed (i.e. transects spaced 10 km apart, and MRDS) should remain as is.

Given that our simulation modelling found a geographical relationship between the aerial survey KDE and spotlighting KDE, here on we focus on determining if the spotlight effort is sufficient as a means of estimating deer abundance and whether effort should be increased or decreased.

We used the average group size, its associated SD, the MR probability and SD and aerial survey density estimates from MRDS, to provide inputs into the simulations. We assumed

the spotlighting ESW was 151 metres (75.5 m either side of the vehicle). We then simulated the likely CV using the current effort of spotlighting in FD1.

Using 2,000 simulations, the CV was estimated to be 38.5%. When we doubled the effort in the simulations, that is we repeated the spotlight transects a second time, the CV reduced to 27.3%. This suggests that in order for spotlighting to provide population estimates with CVs below the commonly used acceptable figure of 25%, spotlighting effort should be doubled (e.g. one repeat survey), together with a small increase in the number of transect lines.

4.0 Discussion

Key findings

The overall purpose of this survey was to produce baseline population estimates for fallow deer and forester kangaroos. Using aerial survey data, we estimated fallow deer using the MRDS approach and kangaroo abundance using the MCDS approach.

For fallow deer, the best performing model, i.e. with the lowest AIC score, was **$g(\mathbf{x}) \sim \text{trainee} + \text{cluster size mr}() \sim \text{trainee} + \text{cluster size} + \text{distance}$** . This suggests that in addition to sightability decaying with distance out from the aircraft, other covariates were affecting heterogeneity in our sightings. These were **cluster size** (i.e. the number of deer clustered together in a group) and the inclusion of count data from the **trainee** observer. For **cluster size**, unsurprisingly, we found sightability increased when there were larger groups of deer. The **trainee** covariate simply flags when a trainee was present. The model suggests the trainee's presence did affect sightability, which if not explicitly dealt with, would have biased the results. In other words, explicitly modelling both of these covariates allowed us to effectively reduce the influence of these biases in the final results. The MRDS model estimated the population of fallow deer to be 53,660, with a CV (i.e. the percentage error estimate) of 19%.

Interestingly, Potts *et al.* (2014) suggested a conservative population estimate of 40,000 fallow deer at the time of their study. Using the spotlight data (corrected for dry conditions and calibrated to our 2019 aerial survey abundance of 53,660), and working back in time to the start of 2014, our calculations suggest that the population could have been 51,058 fallow deer (Figure 11). This is in line with Potts *et al.*'s (2014) general observations.

For forester kangaroos, we estimated population size using the MCDS approach, based only on count data from the front-left and rear-right observers since the trainee observer did not count kangaroos. This gave an estimate of 30,327 forester kangaroos = +/- 23% CV.

By way of comparison only we also trialled a method that brings together the front-left and rear-left seat statistics independently, for a proportion of the full survey when the trainee was not present. This enabled us to estimate the mark-recapture probability, or $p(0)$, at least for that part of the survey. Multiplying the invert of $p(0)$ by 30,237 almost doubled the population estimate of foresters. However, this approach is in essence an extrapolation and

assumes the flight conditions and perception biases are constant throughout. The mark-recapture probability for foresters was quite low ($p(0) = 0.493 \pm 0.10\%$ CV), and in our experience lower than we have encountered elsewhere for aerial kangaroo surveys. Interestingly, for fallow deer the mark-recapture probability was much higher at $p(0) = 0.687 \pm 10\%$ CV. It is possible that this is because on some occasions Forester's may have been mistaken for Bennett's wallabies, leading to discrepancies between the front and rear observers, which would lower $p(0)$. However, trained observers were well briefed about the two species and familiar with their visual differences. Discussions about their differences also occurred early in the survey. Moreover, the two species had a very different build, colouration and movement behaviour. When Bennett's wallabies responded to aircraft noise they quickly dived into the nearest canopy, whereas foresters kept moving. Instead the low $p(0)$ is likely to have arisen because there were not enough sightings and we surmise that had kangaroos been counted by the rear-left observer for 100% rather than 70% of the flights, we may have been able to calculate a more robust estimate of $p(0)$ for foresters, as we did for deer using the full MRDS. For this reason, we suggest that the estimated population of forester kangaroos is at least 30,237 but possibly up to 50% higher. We are not confident it is double 30,237.

As previously mentioned, since the walking transect data for forester kangaroos was over a very small area of the aerial survey it was decided not to attempt to calibrate these data using the aerial survey data as we had done for deer.

Issues encountered

Avoidance behaviour (i.e. animals moving away from the aircraft) was clearly evident during the survey for both species but more prominent with forester kangaroos. This flushing effect is thought to be mainly due to the noise of the aircraft, and lowers the expected detections in viewing zone 1. This is a known problem that potentially violates an important mathematical assumption of MCDS and MRDS, where sightability must always decline with an increased perpendicular distance out from the aircraft (Buckland et al. 2001). With the exception of the trainee, all other observers in this survey were trained with years of experience, and all made a concerted effort to minimise the influence of this effect by regularly looking down into zone 1 and forward of the aircraft.

While more recent methods attempt to deal with this assumption (e.g. see Miller and Thomas 2015), many have used a method called data truncation to effectively remove the zone 1 sightings and, if appropriate, re-adjust the distances measured to other animals further out accordingly. However, Marques (2016) warns that data truncation should only be used when there is reason to believe there is an issue in detectability (observation bias), not animal movement (process variation – Hilborn and Mangel 1997). Marques (2016) suggests that if truncation (e.g. the removal of zone 1) was used to address flushing, it could potentially inflate density estimation because more animals would be observed over a shorter range of distances in the remaining zones (in our case, zones 2–5). Put simply, a systematic bias needs to be present in the data to justify truncation. We did not apply this correction because our observers were trained to be attentive to zone 1 and looking ahead and we believed there was sufficient evidence that the animals were flushed as a result of

the presence of the helicopter. Instead we ensured the models we used (the lines of best fit though the data) smoothed out these effects so that it evened out the slightly higher counts in zone 2 with the slightly lower counts in zone 1. The half-normal $g(x)$ function achieved that for fallow deer, while for foresters the hazard rate $g(x)$ function achieved this (see Marques 2016).

We agree in principle with Marques (2016) that removal of zone 1 counts may inflate population estimates if animal flushing occurred, but with one caveat. The exception we suggest is that, if on average, all animals across all zones were flushed the same amount, and in the same direction, truncation would have been more appropriate. This is because the relative positions of all animals (perpendicular out from the aircraft) would remain approximately fixed, thus constituting a systematic bias in their distance to aircraft position, rather than being process variation as described by Marques (2016).

In fact we did see animals much further out being flushed but are not able to present quantitative evidence to support this observation. In future for manned helicopter surveys where this effect may be apparent, we suggest a colour wide-angle video camera may be a good way to measure the nature of flushing of the animals, thus determining the correct way to manage the problem. Another potential response other than truncation would be to move all zones further out from the aircraft and may be warranted in future aerial surveys in Tasmania.

There was a small detectability bias evident for observers located in the front seat position, which is apparent in Figures 7 and 8. Here the front pillar of the door to the helicopter may have at times distracted the observer's forward-looking view. We consider this a minor problem because our analyses did not indicate that seat position was an important covariate.

At times fallow deer were found in large groups. This can potentially violate the assumption of independent detection between the front and rear observers using MRDS and in circumstances where there are larger groups, they may in fact be under-counted and not over-counted (Clement et al. 2017). Instead Royle (2004) offers an alternative approach combining an MRDS model with an N-mixture model to account for imperfect detection of individuals to reduce these potential biases. We did not test their approach but future research and some investigation of this issue (through simulation modelling) may be worthwhile.

Population growth rate of fallow deer

We did not have the luxury of a time series of both spotlight surveys and aerial surveys to analyse how they compare over time. Instead we used KDE surfaces in geographical space of both the 2019 spotlighting data (measured as deer per linear km) and the 2019 aerial survey (measured as deer per km²), which were collected two months apart, to conduct a geographical comparison, rather than temporal comparison of the two. A temporal comparison would be ideal in the long-term but we acknowledge it would be expensive to

fly a helicopter over the whole area every year. We sought to find a scale factor (an indirect estimate of ESW) for the spotlighting surveys, using the aerial survey data. This assumes there were no systematic errors in the aerial survey data. Without knowing the true population, it would be difficult to detect systematic biases in the aerial survey unless aerial surveys were undertaken over a 12 month period and compared with reported takes.

Interestingly, in the presence of hunting and a severe drought in 2000, the DPIWE (2011) reported a net population increase of about 4.6% per annum between 1972 and 1990. This closely agrees with our estimated net population growth rate of 5.4% for deer, using the spotlight transects from 2006–2019, corrected for dry condition effects. However, this is only approximate and is not the natural population growth rate in the absence of removals. Like Potts *et al.* (2014) we suggest there is no evidence of density dependency (i.e. slowing of population growth due to food resource limitations).

Hone *et al.* (2010) used demographic data, specifically the female age at first reproduction, to estimate maximum population growth rates of a naturally increasing population of fallow deer. Their estimated maximum population growth rate (i.e. when resources are not limiting, and there is no hunting, predators, parasites, or competitors) was $r_m = 0.45$ (0.13–1.18, 95% CI). The exponent of this is 1.583. This equates to a 56.8% increase per annum. However, observations in the south-east of South Australia indicate that this figure is high and 30% is more likely for fallow deer (MacKenzie *pers. comm.* 2014). Using 2006–2019 Tasmanian deer spotlighting data, corrected for dry condition effects and largely removing the effects of removals on population growth, we produced a similar natural population growth rate of around 27% per annum. Because removals will alter the demographic structure of fallow deer, this estimate is only approximate and is likely to be downwardly biased.

Thermal technology

The experimental results of the thermal camera trial are presented in Appendix 5. The thermal camera imagery did not allow the desktop observer to distinguish Bennett's wallabies (*Macropus rufogriseus*) from forester kangaroos (*M. giganteus tasmaniensis*). Developing techniques for distinguishing between similar species would be needed before this technology could be used to estimate forester kangaroo populations in Tasmania. [might warrant a mention here of how well it works in other places where similar-sized macropods are sympatric]

When suspected fallow deer were not clear enough in the imagery to be sure, we excluded them. This gave a final abundance estimate for fallow deer in FD1 of 56,150. This is 2,490 higher than the estimate produced via MRDS.

Of the remaining animals seen in the imagery, 22% could not be correctly identified as either deer or macropods. Thus some of these unknown animals may have been deer. If these unknowns could be identified more clearly, this might have increased the estimated number of deer using the thermal technology.

For this reason alone, we are not yet convinced that thermal technology is currently suitable for use from a helicopter or aeroplane. We have previously worked with higher resolution thermal cameras in helicopters, including a Vayu HD thermal camera. This also has an uncooled microbolometer sensor, capable of recording 1920 x 1200 pixels at 30 frames per second. But our analysis of this camera was in landscapes of mainly in open grasslands or shrublands, and we suggest this camera would not have reduced the remaining 22% of unknown sightings. While some authors offer de-blurring detection algorithms (Zhu et al 2010) and multiple frame overlaying and sharpening approaches (all with the potential to be applied to thermal imagery), in our experience these are most likely to only work in improving animal detection in open areas.

The reason for the high percentage of unknown species is that motion blur was apparent in the data, confounded further in wooded areas. Motion blur is not an issue that can be solved purely by faster video frame rates. Camera gimbals and stabilisers only partly remove its effects. Motion blur (sometimes referred to as ground blur) is a phenomenon that is primarily the product of aircraft height and aircraft speed. Even with a higher resolution camera, an aircraft flown too high would not allow the side profile of the animal to be deciphered, which is important in classifying the animal. Given that it is unsafe and not cost-effective to fly a helicopter as slow as 30 knots, a large number of experiments have now been conducted by the authors (yet unpublished) using several Unmanned Aerial Vehicles (UAVs) flown at night as slow as 30 knots. This provides much sharper images of wildlife, allowing many species to be deciphered.

We also considered using the thermal imaging as a “fourth observer” and undertake a separate MRDS between the right-rear observer and the camera located on the right-hand side of the aircraft. Even if the 22% uncertainty in species classification we encountered could be reduced significantly, Broker et al found significant inaccuracies in combining a human observer with a camera in MRDS, together with unrealistic abundances and confidence intervals. While they suggest more precise timing between human and camera observations might reduce these inaccuracies, we

However, thermal technology will not (nor may never) allow one to distinguish between species within most genus groupings and this will remain its largest limitation, well into the future.

5.0 Recommendations and future work

The role of spotlight transects

Using simulation modelling, and based on current information, if the spotlighting effort were at least doubled in effort, a CV of under 25% is likely to be achievable. Because in each simulation, the animals are redistributed according to the KDE density map, it does not provide any insights about where to best increase the spotlighting effort. Assuming the

animals are mobile and randomly moving in and out of view of the spotlight transect lines, doubling the effort this could be achieved by simply repeat-sampling the same transects over more than one night. However, it may be more productive to increase the number of transects, thus increasing their geographical distribution and statistically stratifying them in different habitats. Otherwise there is a risk that resampling the same transects will not provide independent results or be representative of all habitat types. Moreover, future design planning should look more closely at their current stratification and how this could also be improved.

In this study, we used a coarse and indirect method to calculate the effective strip width of the spotlighting surveys by determining the scale factor that relates deer per kilometre length estimates from spotlighting with deer per square kilometre estimates from the aerial survey. Put simply, if length (in kilometres) multiplied by width (in kilometres) is kilometres squared, then the average deer per kilometre, multiplied by this scale factor gives deer per kilometres squared. We needed to do this to be able to coarsely analyse fallow deer trends over time but ideally the spotlight surveys in future should employ distance sampling, including recording covariates such as vegetation density, so that MCDS could be applied to the spotlighting data. This also allows a CV to be estimated, together with a more robust ESW.

In summary, improving the spotlight transect sampling would allow aerial surveys to be conducted less frequently, say at 4 - 5-year intervals, with a primary role of validating and re-calibrating the spotlight transect data.

As we had little ground survey data about forester kangaroos that would have allowed a comparison between population counts obtained from ground versus aerial surveys, it is difficult to make similar recommendations for the future monitoring of forester kangaroos. We suggest that the degree of agreement between ground and aerial counts of foresters requires further research, and the best way forward would be to compare a range of survey methods over one or two trial areas (see below).

Other forms of monitoring

The use of UAVs in aerial surveys is expanding rapidly and in addition to the benefits of aircraft safety in undulating and hazardous terrain, these systems are potentially more cost-effective and have potentially higher detection rates (see below), with less disturbance to wildlife (Broker et al 2019). UAVs with thermal cameras are able to detect and identify animals but under certain flying conditions (Sharp 2015). Following work carried out by Israel (2011) with deer, Lethbridge et al. (2020) compared MCDS densities of feral pigs using UAV thermal imagery with helicopter thermal imagery flown during the day, in low shrubland and woodland areas along the Lachlan River in NSW. They estimated similar, and at times higher densities using a UAV flown at night. Over several years, a UAV has also been successfully used by the authors to count Western Grey kangaroos in the Coorong National Park in SA.

We therefore suggest flying a UAV over a sub-set of spotlight transects as an experiment to test the cost-benefits of this technology versus ground surveys. However, while Beyond Visual Line of Sight (BVLoS) applications to the Civil Aviation Safety Authority (CASA) could be approved over smaller areas, it is unlikely that a UAV flying BVLoS over a third of Tasmania would be approved, let alone cost-effective. We suggest that UAVs would be better placed to fly over smaller areas of under 15 x 15 km, and if proven, could be more useful in remote areas of Tasmania.

To be able to employ MCDS, Lethbridge (2019) stress the need to install two thermal cameras in the UAV and face them perpendicular to the flight direction. Two cameras are necessary to be cost-effective because it doubles the sample size for the same flight. As thermal imagery from the UAV may not be able to distinguish which macropod species, it may need to be combined with one (or more) ground survey methods, such as spotlighting, walking transects or camera trapping to provide a rudimentary ratio of species to the camera counts or be integrated using a more elaborate modelling approach.

In addition to the application described above, camera traps may also be useful in their own right in low density areas of deer and forester kangaroos, providing they are carefully placed and there are a sufficient number of cameras installed. In these areas they can be left for long periods of time for early-warning detection or for measuring the infrequent use of habitats by these animals.

Thermal binoculars

The application of thermal binoculars in walking transects or stop-start vehicle transects is still in its infancy and there is no mention of this in key literature such as Sharp (2015), mainly because the advancement of this technology has only occurred in the last three years. While as yet unpublished, an extensive study by the authors has shown the use of quality thermal binoculars with rangefinders in animal detection at night (using MCDS) has great promise. In the Coorong National Park SA, and together with Mr Alex Nankivell from Nature Foundation in the Gawler Ranges SA, the authors have compared results from thermal binoculars at night with day walking transects, driving transects, and UAV surveys over the same areas. Early indications show they compare well with UAV thermography at night and both density estimates from these technologies are significantly higher than those using employing MCDS during the day. As the use of this technology is still in its infancy, we suggest that to begin with, a research study in Tasmania could be used to compare this with the current spotlighting approach and possibly a UAV MCDS approach over the same pilot area(s).

Density maps

In the absence of other information, we used the Kernel Density Estimator to create a density surface through the sample of point locations of fallow deer and forester kangaroos. However, improvements to the density distribution maps would be possible if correlations could be found between these species and their landscape, should more detailed data about

the vegetation, environmental conditions and terrain be available. For example, Herr et al (2019) used MRDS data to estimate the density of Antarctic minke (*Balaenoptera bonaerensis*) whales and then tested for correlations between their point sample data and the habitat characteristics of this species. They then used Generalised Additive Models (a form of regression) to produce more detailed distribution maps of this species of *B. bonaerensis*.

6.0 References

- Akaike, H. 1974, 'A new look at the statistical model identification', *IEEE Transactions on Automatic Control*, 19 (6): 716–723.
- Bayliss, P. 1985, 'The population dynamics of red and western grey kangaroos in arid New South Wales, Australia. I. Population Trends and Rainfall', *Journal of Animal Ecology*, 54: 111-25.
- Bayliss, P. 1987. *Kangaroo dynamics*. In 'Kangaroos: their Ecology and Management in the Sheep Rangelands of Australia', Eds G. Caughley, N. Shepherd and J. Short. Cambridge University Press, pp. 119–134.
- Becker, E.F. and Christ, A.M. 2015, 'A unimodal model for double observer distance sampling Surveys', *PLoS One*, 10(8).
- Borchers, D.L., Zucchini, W., and Fewster, R.M. 1998, 'Mark-recapture models for line transect surveys', *Biometrics*, 54(4): 1207-1220.
- Borchers, D. L., Laake, J. L., Southwell, C., and Paxton, C. G. M. 2006. 'Accommodating Unmodeled Heterogeneity in Double-Observer Distance Sampling Surveys', *Biometrics*, 62: 372–378.
- Broker K., Hansen, R., Leonard, K. Koski, W. and Heide-Jørgensen, M.P. 2019. A comparison of image and observer based aerial surveys of narwhal: AERIAL SURVEYS OF NARWHAL. *Marine Mammal Science*. 10.1111/mms.12586.
- Buckland, S. T. 2001, 'Shipboard sightings surveys: methodological developments to meet practical needs', in Bulletin of the International Statistical Institute, 53rd Session Proceedings, ed. pp. 315-318.
- Buckland, S. T., Anderson, D. R., Burnham, K. P. & Laake, J. L. 1993, *Distance Sampling: Estimating Abundance of Biological Populations*, Chapman and Hall, London.
- Burt, M. L., Borchers, D. L., Jenkins, K. J., and Marques, T. A. 2014, 'Using mark–recapture distance sampling methods on line transect surveys', *Methods in Ecology and Evolution*, 5: 1180–1191.

- Caughley, J., Bayliss, P., and Giles, J. 1984, 'Trends in kangaroo numbers in western New South Wales and their relation to rainfall', *Australian Wildlife Research*, 11: 415-22.
- Caughley, G., Grigg, G. C., and Smith, L. 1985, 'The effect of drought on kangaroo populations', *Journal of Wildlife Management*, 49: 679-85.
- Driessen, M.M., and Hocking, G. J. 1992. 'Review and Analysis of Spotlight Surveys in Tasmania: 1975-1990'. Department of Parks, Wildlife and Heritage, Tasmania, Scientific Report, 92/1.
- Edwards, G. P., Saalfeld, K. and Clifford, N. 2004. Population trend of feral Camels in the Northern Territory, Australia, *Wildlife Research*, vol. 31, pp. 509-517.
- Fewster R.M., Pople A.R. 2008, 'A comparison of mark-recapture distance-sampling methods applied to aerial surveys of eastern grey kangaroos', *Wildlife Research*, 35: 320-330.
- Fotheringham, A.S. Brunsdon, C. Charlton M. 2002 Geographically Weighted Regression: The Analysis of Spatially Varying Relationships. Wiley.
- Herr, H., Kelly, N., Dorschel, B., Huntemann, M., Kock, K. H., Lehnert, L. S., Siebert, U., Viquerat, S., Williams, R., & Scheidat, M. 2019. Aerial surveys for Antarctic minke whales (*Balaenoptera bonaerensis*) reveal sea ice dependent distribution patterns. *Ecology and evolution*, 9(10), 5664-5682.
- Hilborn R. & M. Mangel M. 1997. The Ecological Detective: Confronting Models with Data. Princeton University Press, Princeton, New Jersey
- Hone, J., Duncan, R. and Forsyth, D. 2010, 'Estimates of maximum annual population growth rates of mammals and their application in wildlife management', *Journal of Applied Ecology*, vol. 47, pp. 507-14.
- Israel, M., 2011. A UAV-based roe deer fawn detection system. Int. Arch. Photogram. Remote Sens. Spatial Inform. Sci, vol. XXXVIII-1/C22, ISPRS Zurich 2011 Workshop, Sept. 14-16, 2011, Zurich, Switzerland.
- Ivlev, V. S. 1961, *Experimental ecology of the feeding of fishes*. Yale University Press, New Haven.
- Laake, J. L. and Borchers, D. L. 2004, *Methods for incomplete detection at distance zero*, In 'Advanced Distance Sampling', Eds S. T. Buckland, D. R. Anderson, K. P. Burnham, J. L. Laake, D. L. Borchers and L. Thomas, Oxford Univ. Press, Oxford, United Kingdom, pp. 108-189.

- Laake, J., Dawson, M. J., & Hone, J. 2008. Visibility bias in aerial survey: Mark–recapture, line- transect or both? *Wildlife Research*, 35, 299–309.
- Lande, R., Engen, S. and Sæther, B. E. 2009. An evolutionary maximum principle for density-dependent population dynamics in a fluctuating environment. *Philosophical transactions of the Royal Society of London. Series B, Biological sciences*, 364(1523), 1511–1518.
- Lande, R., Engen S., Sæther B. 2003 *Stochastic Population Dynamics in Ecology and Conservation*, Oxford University Press.
- Lethbridge, M. 2015. *Aerial and ground survey CV simulator*, Software.
- Lethbridge MR, 2018, *Feral Deer Aerial Survey of Gum Lagoon Conservation Park and an Unmanned Aerial Vehicle evaluation, 2018*. Report to Upper South East District | Parks & Regions, Department of Environment, Water and Natural Resources, South Australia.
- Lethbridge, M.R. 2019 *Program Thermal*. Software.
- Lethbridge, M.R., Stead, M.G. and Wells, C. 2019, 'Estimating kangaroo density by aerial survey: a comparison of thermal cameras with human observers', *Wildlife Research*, vol. 46, pp. 639–648
- Lethbridge, M.R., Wells, C.R., Stead, M.G. 2020. NSW Thermal Camera Pig Survey 2020 and Removal Operations Analysis, EcoKnowledge, South Australia.
- Marques, T. A. 2016, 'A comment on Horcajada-Sánchez and Barja (2015): a cautionary tale about left truncation and density gradients in distance sampling', *Annales Zoologici Fennici*, 53: 52–54.
- Marsh, H. and Sinclair, D. F. 1989. 'Correcting for visibility bias in strip transect aerial surveys of aquatic fauna', *Journal of Wildlife Management*, vol. 53, no. pp. 1017-1024.
- Marshall, L. 2020. Package 'DSsim' Version 1.1.5. Software for the Statistical package R.
- McCullum H. 2000. 'Population Parameters. Estimation for Ecological Models', Blackwell, Oxford.
- Miller D.L., Thomas L. 2015. Mixture Models for Distance Sampling Detection Functions. *PLoS ONE* 10(3).
- Newsome, A. E. 1965a, 'The abundance of red kangaroos, *Megaleia rufa* (Desmarest), in central Australia', *Australian Journal of Zoology*, 13: 269-87.

- Newsome, A. E. 1965b. 'The distribution of red kangaroos, *Megaleia rufa* (Desmarest), about sources of persistent food and water in central Australia', *Australian Journal of Zoology*, 13: 289-99.
- Newsome, A. E., Stephens, D. R., and Shipway, A. K. 1967, 'Effect of a long drought on the abundance of red kangaroos in central Australia', *CSIRO Wildlife Research*, 12: 1-8.
- Pollock, K. H. and Kendall, W. L. 1987. 'Visibility bias in aerial surveys: A review of estimation procedures', *Journal of Wildlife Management*, vol. 51, no. pp. 501-509.
- Ratcliffe, J.H. McCullagh M.J. 1999. Hotbeds of crime and the search for spatial accuracy. *Journal of Geographical Systems*. 1: 385-398 Springer-Verlag.
- Royle, J. A. 2004. N- mixture models for estimating population size from spatially replicated counts. *Biometrics*, 60, 108–115
- Sharp, E.J. Thermal Imaging Techniques to Survey and Monitor Animals in the Wild: A Methodology. 2015.
- Samuel, M. D., Garton, E. O., Schlegel, M. W. and Carson, R. G. 1987. 'Visibility bias during aerial survey of Elk in north central Idaho', *Journal of Wildlife Management*, vol. 51, no. pp. 622-630.
- Seber, G. A. F. 1982. *The estimation of Animal Abundance and Related Parameters*, Charles Griffin & Company Ltd., New York.
- Silverman, B.W. 1986, *Density Estimation for Statistics and Data Analysis*, Chapman and Hall, London.
- Thomas, L., S.T. Buckland, E.A. Rexstad, J. L. Laake, S. Strindberg, S. L. Hedley, J. R.B. Bishop, T. A. Marques, and K. P. Burnham. 2010. Distance software: design and analysis of distance sampling surveys for estimating population size. *Journal of Applied Ecology* 47: 5-14.
- Woodall, P.F. 1983, 'Distribution and population dynamics of dingoes (*Canis familiaris*) and feral pigs (*Sus scrofa*) in Queensland, 1945–1976', *Journal of Applied Ecology*, 20: 85–95.
- Zhu, H. Liu, M. Ji, H. and Li, Y. 2010. Combined invariants to blur and rotation using Zernike moment descriptors. *Journal of Pattern Analytical Applications* 13:309-319